JOURNAL OF Materials CHEMISTRY

Synthesis and crystal structures of two new titanium alkoxy–diolate complexes. Potential precursors for oxide ceramics

Anthony C. Jones,*[a,b] Paul A. Williams,[a] Jamie F. Bickley,[a] Alexander Steiner,[a] Hywel O. Davies,[b] Timothy J. Leedham,[b] Amir Awaluddin,[c] Martyn E. Pemble[c] and Gary W. Critchlow[d]

[a]*Department of Chemistry, University of Liverpool, Liverpool, UK L69 7ZD*
[b]*Inorgtech Limited, 25 James Carter Road, Mildenhall, Suffolk, UK IP28 7DE*
[c]*Department of Chemistry, University of Salford, Salford, UK M5 4WT*
[d]*Institute of Surface Science and Technology, University of Loughborough, Loughborough, Leicestershire, UK LE11 3TU*

Received 10th January 2001, Accepted 1st March 2001
First published as an Advance Article on the web 3rd April 2001

The new titanium alkoxy–diolate precursors $[Ti(OCH_2CH_2O)(OCH_2CH_2NMe_2)_2]_2$ (**1**) and $[Ti(OCMe_2CMe_2O)(OCH_2CH_2NMe_2)_2]_2$ (**2**) have been prepared and structurally characterised by single crystal X-ray diffraction. Both compounds exhibit binuclear centrosymmetric structures with bridging alkoxide groups, containing two six-coordinate Ti atoms in distorted octahedral environments. In (**1**) the oxygen from the ethylene glycolate ligand is involved in bridging, whereas in (**2**) the bridging oxygen is provided by the dimethylamino ethoxide ligand. Complexes (**1**) and (**2**) are potential precursors for Ti-containing oxides and both complexes have been investigated as precursors for the deposition of TiO_2 thin films by liquid injection metalorganic chemical vapour deposition (MOCVD). Significantly, only complex (**2**) led to reproducible TiO_2 deposition in the temperature range 325–450 °C, whilst complex (**1**) exhibited a marked pre-reaction leading to highly irreproducible film growth. The difference in MOCVD behaviour between the complexes is rationalised in terms of their molecular structure.

1. Introduction

Titanium alkoxides have a wide variety of industrial applications, such as catalysts in the manufacture of esters and polyolefins,[1] in asymmetric organic synthesis using the Katsuki–Sharpless epoxidation procedure,[2] and as precursors in the sol–gel deposition of mesoporous titanium(IV) oxides and titania–silica catalysts.[3] They are also precursors to a range of important electroceramic materials deposited by sol–gel techniques[4] or metalorganic chemical vapour deposition (MOCVD).[5,6] These include $SrTiO_3$ and $(Ba,Sr)TiO_3$ high-k dielectric layers for DRAM applications, and $Pb(Zr,Ti)O_3$ ferroelectric films used in infrared detectors or FERAM computer memories.[7]

The structure of the titanium alkoxide precursor plays a crucial role in determining the chemistry of sol–gel or MOCVD deposition processes. For instance, the high susceptibility of $[Ti(OR)_4]$ (R = alkyl, aryl) species to hydrolysis can be problematic in sol–gel processes,[4] leading to premature precipitation of insoluble oxo species. Various bidentate/chelating ligands such as acetic acid[8] and acetylacetone[9] have therefore been added to modify and control the reactivity of the titanium alkoxide by increasing the coordinative saturation around the Ti centre.

$Ti(OR)_4$ precursors are also susceptible to pre-reaction in MOCVD reactors and their high moisture sensitivity makes them difficult to use in solution-based liquid injection MOCVD, which is being increasingly used for the deposition of dielectric and ferroelectric metal oxides.[10] There is also the possibility of pre-reaction between $Ti(OR)_4$ and other precursors in multi-component solutions. Therefore, modified alkoxides such as $[Ti(OPr^i)_2(thd)_2]$[11,12] (thd = 2,2,6,6-tetramethylheptane-3,5-dionate) and $[Ti(OPr^i)_2(dmae)_2]$[13,14] (dmae = *N*,*N*′-dimethylaminoethoxide, $OCH_2CH_2NMe_2$) which have an increased coordinative saturation at the metal centre have been used as alternatives to $Ti(OR)_4$ in liquid injection MOCVD.

In addition to imparting higher ambient stability to the Ti alkoxide, the insertion of the [dmae] ligand in a titanium alkoxide has also been claimed[15] to lead to more uniform oxide layer growth, and $Ti(dmae)_4$ has recently been used for the liquid injection MOCVD of $(Ba,Sr)TiO_3$.[15] $(Ba,Sr)TiO_3$ has also been deposited by liquid injection MOCVD using a titanium β-diketonate–diolate complex, $[Ti(mpd)(thd)_2]$ (mpd = 2-methylpentane-2,4-diolate)[16] and this has led us to investigate mixed diolate–dmae complexes of titanium, $[Ti(diol)(dmae)_2]$, as liquid injection MOCVD precursors. These were expected to contain a fully saturated six-coordinate Ti centre making them more stable than $Ti(OR)_4$ compounds in solution. The presence of the [diolate] and [dmae] ligands is also expected to facilitate the growth of high quality TiO_2 at the relatively low substrate temperatures (< 550 °C) required for microelectronics applications. Complexes of the type $[Ti(diol)(dmae)_2]$ may also have wider industrial applications, as mixtures of titanium alkoxides and glycols have been used as water-proofing agents, surface coatings and adhesives.[17]

A number of heteroleptic titanium alkoxy–diolate complexes have been reported, including $[Ti(OCH_2CH_2O)(OR)_2]$ (R = Et, Pr^i, Bu^t),[18] $[Ti[(CH_3)_2C(O)CH_2CH(O)CH_3](OR)_2]$,[19] $[Ti(mpd)(OR)_2]$ (R = Et, Pr^n, Bu^n, $Pent^n$)[20] However, in much of this early work the compounds are often poorly characterised and structural data are absent. More recently, the homoleptic Ti–diolates $[Ti(OCH_2CH_2O)]_n$[21] and $[Ti(dmpd)_2]_2$ (dmpd = 2,4-dimethylpentane-2,4-diolate).[22] have been structurally charac-

 DOI: 10.1039/b100411p

terised. In this paper the crystal structures of the new alkoxy–diolate precursors $[Ti(OCH_2CH_2O)(OCH_2CH_2NMe_2)_2]_2$ (**1**) and $[Ti(OCMe_2CMe_2O)(OCH_2CH_2NMe_2)_2]_2$ (**2**) are reported, and studies into the liquid injection MOCVD of TiO_2 thin films using (**1**) and (**2**) are presented.

2. Experimental

General techniques

All syntheses were carried out in an inert atmosphere of nitrogen using a glovebox or standard Schlenk line techniques. Titanium tetra-isopropoxide $Ti(OPr^i)_4$ (99.9%) was supplied by Inorgtech and was used without further purification. Toluene, ethylene glycol ($HOCH_2CH_2OH$), pinacol ($HOCMe_2CMe_2OH$), and *N*,*N*′-dimethylaminoethanol ($HOCH_2CH_2NMe_2$), were obtained from Aldrich Chemical Co. and were dried by conventional methods and degassed before use.

^1H NMR spectra were recorded on a Bruker 300 NMR spectrometer using the proton impurities of the deuterated benzene solvent as a reference, and the $^{13}C\{^1H\}$ resonance of the solvent as reference in the $^{13}C\{^1H\}$ spectra. All chemical shifts are reported positive to the high frequency of the standard. Infrared spectra were recorded on a Perkin Elmer 177 spectrometer using Nujol mulls between NaCl plates. Elemental microanalyses were performed by the Chemistry Department service of Liverpool University.

Auger electron spectroscopy was carried out on a Varian scanning Auger spectrometer. The atomic compositions quoted are from the bulk of the film, free from surface contamination and were obtained by combining AES with sequential argon ion bombardment until comparable compositions were obtained for consecutive data points. Compositions were based on an un-sputtered and sputtered TiO_2 powder reference material for surface and bulk data respectively. Depth scale calibration for estimating film thickness was achieved using an experimentally derived etch rate from PVD-deposited TiO_2 on glass (optical coating).

X-Ray diffraction on the TiO_2 films was carried out using a Siemens D5000 difractometer using Cu-Kα radiation.

Precursor synthesis

$[Ti(OCH_2CH_2O)(OCH_2CH_2NMe_2)_2]_2$ (1). Ethylene glycol, $HOCH_2CH_2OH$ (1.05 g, 16.9 mmol) was added to $Ti(OPr^i)_4$ (4.80 g, 16.9 mmol) with stirring. The mixture initially became cloudy and evolved heat before returning to a clear colourless liquid. The mixture was stirred for 30 min and then volatiles were removed *in vacuo* to yield $[Ti(OCH_2CH_2O)(OPr^i)_2]$ as a viscous clear colourless liquid.

N,*N*′-Dimethylaminoethanol (dmaeH), $HOCH_2CH_2NMe_2$ (3.02 g, 33.9 mmol) was then added with stirring to a solution of $[Ti(OCH_2CH_2O)(OPr^i)_2]$ (3.82 g, 16.9 mmol) in toluene ($\sim$20 cm^3). The solution was boiled under reflux for one hour and then allowed to cool. Volatiles were removed *in vacuo* to give a white solid. This was re-dissolved in the minimum quantity of hot toluene and left overnight at -15 °C to give $[Ti(OCH_2CH_2O)(OCH_2CH_2NMe_2)_2]_2$ as air-sensitive colourless crystals. Yield: 2.18 g, 45.3%.

Anal. Calc. for $C_{20}H_{48}N_4O_8Ti_2$: C, 42.3; H, 8.5; N, 9.9. Found: C, 42.7; H, 8.5; N, 9.6%.

^1H NMR (C_6D_6, 30 °C): δ 2.30 [32H, m, $OCH_2CH_2N(CH_3)_2$], 4.47 [8H, s, OCH_2CH_2O], 4.55 [8H, t, $OCH_2CH_2N(CH_3)_2$]; $^3J_{HH}=5.8$ Hz.

$^{13}C\{^1H\}$ NMR (C_6D_6, 30 °C): δ 45.7 [$OCH_2CH_2N(CH_3)_2$], 62.8 [$OCH_2CH_2N(CH_3)_2$], 71.5 [$OCH_2CH_2N(CH_3)_2$], 75.7 [OCH_2CH_2O].

IR (Nujol, cm^{-1}) 1317 w, 1266 w, 1231 w, 1178 w, 1160 w, 1077 w, 1041 vs, 1025 m, 948 m, 905 m, 879 m, 863 w, 786 w, 722 w, 665 s, 645 vs.

$[Ti(OCMe_2CMe_2O)(OCH_2CH_2NMe_2)_2]_2$ (2). $Ti(OPr^i)_4$ (4.83 g, 17.0 mmol) was added with stirring to pinacol, $HOCMe_2CMe_2OH$ (2.01 g, 17.0 mmol), which dissolved slowly with the evolution of heat to give a milky white solution. The mixture was then gently heated until it became clear and colourless and was then allowed to cool. All volatiles were removed *in vacuo* to give $[Ti(OCMe_2CMe_2O)(OPr^i)_2]$ as a white solid.

$HOCH_2CH_2NMe_2$ (3.03 g, 34.0 mmol) was then added to a stirred solution of $[Ti(OCMe_2CMe_2O)(OPr^i)_2]$ (3.09 g, 17 mmol) in toluene ($\sim$20 cm^3). The resulting pale yellow solution was boiled under reflux for 1 h, and then all volatiles were removed *in vacuo* to give a pale yellow solid. This was then re-dissolved in the minimum quantity of hot toluene and left overnight at -15 °C to give $[Ti(OCMe_2CMe_2O)(OCH_2CH_2NMe_2)_2]_2$ (**2**) as air-sensitive colourless crystals. Yield: 1.92 g, 33.2%.

Anal. Calc for $C_{28}H_{64}N_4O_8Ti_2$: C, 49.4; H, 9.5; N, 8.2. Found: C, 49.8; H, 9.7; N, 7.9%.

^1H NMR (C_6D_6, 30 °C): δ 1.42 [24H, s, $OC(CH_3)_2C(CH_3)_2O$], 2.20 [12H, s, $OCH_2CH_2N(CH_3)_2$], 2.34 [12H, br s, $OCH_2CH_2N(CH_3)_2$], 2.50 [4H, t, $OCH_2CH_2N(CH_3)_2$]; $^3J_{HH}=6.4$ Hz, 2.70 [4H, br, $OCH_2CH_2N(CH_3)_2$], 4.15 [4H, br, $OCH_2CH_2N(CH_3)_2$], δ 4.64 [4H, t, $OCH_2CH_2N(CH_3)_2$]; $^3J_{HH}=6.4$ Hz.

$^{13}C\{^1H\}$ NMR (C_6D_6, 30 °C): δ 27.7 [$(CH_3)_2COCO(CH_3)_2$], 46.1 [$OCH_2CH_2N(CH_3)_2$], 46.6 [$OCH_2CH_2N(CH_3)_2$], 60.1–63.8 [3 peaks, $OCH_2CH_2N(CH_3)_2$], 66.8–74.0 [3 peaks, $OCH_2CH_2N(CH_3)_2$], 94.2 [$(CH_3)_2COCO(CH_3)_2$], 95.1 [$(CH_3)_2COCO(CH_3)_2$].

IR (Nujol, cm^{-1}) 1369 m, 1365 m, 1354 m, 1276 w, 1274 vw, 1191 w, 1154 vs, 1122s, 1103 m, 1083 m, 1064 s, 1047 m, 1029 m, 997 m, 975 vs, 950 m, 908 w, 889 w, 790 w, 779 w, 707 s, 655 s, 641 vs.

Single crystal X-ray diffraction

Crystallographic data for (**1**) and (**2**) were recorded on a STOE-IPDS diffractometer using graphite monochromated Mo-Kα radiation ($\lambda=0.71073$ Å), $T=200$ K, in the ω-rotation mode ($\Delta\omega=2°$). Structures were solved by Direct Methods and refined by full-matrix least squares against F^2 using all data.[23] All-non hydrogen atoms were refined anisotropically. Hydrogen positions were calculated with C–H distances of 0.99 Å (methylene C–H) and 0.98 Å (methyl C–H) and assigned isotropic thermal parameters of $U(H)=1.2U_{eq}(C)$ for methylene H atoms and $U(H)=1.5U_{eq}(C)$ for methyl H atoms (default settings in SHELX97).[23] Crystal and data collection parameters for (**1**) and (**2**) are given in Table 1.

CCDC reference numbers 158131 and 158132. See http://www.rsc.org/suppdata/jm/b1/b100411p/ for crystallographic data in CIF or other electronic format.

MOCVD of TiO_2 thin films

Thin films of TiO_2 were deposited by liquid injection MOCVD using 0.1 molar solutions of $[Ti(OCMe_2CMe_2O)(OCH_2CH_2NMe_2)_2]_2$ (**2**) in tetrahydrofuran (THF). The films were deposited over the temperature range 325–450 °C on to Si(100) single crystal substrates using an atmospheric pressure CVD reactor, similar to one described elsewhere.[24] The growth conditions are summarised in Table 4 (later), together with some analytical results.

3. Results and discussion

Crystallography

The crystal structure of (**1**) is shown in Fig. 1. The complex is binuclear and centrosymmetric, containing two six-coordinate Ti atoms with a $[TiO_5N]$ coordination sphere. The bridging

Table 1 Crystal and data collection parameters for $[Ti(OCH_2CH_2O)(OCH_2CH_2NMe_2)_2]_2$ (**1**) and $[Ti(OCMe_2CMe_2O)(OCH_2CH_2NMe_2)_2]_2$ (**2**)

Compound	(**1**)	(**2**)
Empirical formula	$C_{20}H_{48}N_4O_8Ti_2$	$C_{28}H_{64}N_4O_8Ti_2$
Formula weight	568.52	680.76
a/Å	8.2993(17)	9.3358(14)
b/Å	9.3651(19)	10.0168(16)
c/Å	9.7070(19)	11.4403(18)
α/°	104.70(2)	110.358(17)
β/°	104.99(2)	107.365(18)
γ/°	96.58(2)	99.353(18)
V/Å^3	691.7(2)	913.9(2)
Crystal system	Triclinic	Triclinic
Space group	$P\bar{1}$	$P\bar{1}$
Z	1	1
crystal size/mm	$0.5 \times 0.4 \times 0.2$	$0.4 \times 0.3 \times 0.3$
μ/mm^{-1}	0.624	0.484
Refl. collected	3807	5798
Refl. unique (R_{int})	2063 (0.0478)	2692 (0.0286)
parameters refined	154	190
$R1$ [$I > 2\sigma(I)$]	0.0355	0.0299
$wR2$ (all data)	0.0833	0.0823

Table 2 Selected bond lengths (Å) and angles (°) for (**1**) and (**2**)

(**1**)		(**2**)	
Ti(1)–O(1)	1.836(2)	Ti(1)–O(1)	1.8665(14)
Ti(1)–O(2)	1.8263(18)	Ti(1)–O(2)	1.8768(14)
Ti(1)–O(3)	1.8653(19)	Ti(1)–O(3)	1.8131(15)
Ti(1)–O(4)	2.064(2)	Ti(1)–O(4)	2.0128(13)
Ti(1)–O(4′)	1.9880(17)	Ti(1)–O(4′)	2.0909(13)
Ti(1)–N(1)	2.409(2)	Ti(1)–N(2)	2.3041(17)
O(4′)–Ti(1)–O(4)	70.86(8)	O(4′)–Ti(1)–O(4)	71.07(6)
O(1)–Ti(1)–O(3)	101.43(9)	O(3)–Ti(1)–O(2)	107.98(7)
O(4)–Ti(1)–O(3)	78.46(8)	O(4)–Ti(1)–O(2)	98.69(6)
O(4′)–Ti(1)–O(1)	106.52(9)	O(4′)–Ti(1)–O(3)	92.96(6)
O(2)–Ti(1)–O(1)	93.42(9)	O(1)–Ti(1)–O(2)	80.05(6)
O(2)–Ti(1)–O(4′)	93.74(8)	O(1)–Ti(1)–O(3)	103.43(7)
O(2)–Ti(1)–O(4)	99.88(9)	O(1)–Ti(1)–O(4)	111.22(6)
O(2)–Ti(1)–O(3)	99.34(9)	O(2)–Ti(1)–O(4′)	155.75(6)
O(3)–Ti(1)–O(4′)	148.28(9)	O(3)–Ti(1)–O(4)	139.26(6)
O(1)–Ti(1)–O(4)	166.56(8)	O(1)–Ti(1)–O(4′)	83.37(6)
N(1)–Ti(1)–O(2)	168.15(9)	N(2)–Ti(1)–O(1)	158.50(6)
N(1)–Ti(1)–O(1)	74.98(8)	N(2)–Ti(1)–O(2)	78.51(6)
N(1)–Ti(1)–O(3)	85.61(8)	N(2)–Ti(1)–O(3)	81.88(7)
N(1)–Ti(1)–O(4)	91.64(8)	N(2)–Ti(1)–O(4)	73.79(6)
N(1)–Ti(1)–O(4′)	87.38(7)	N(2)–Ti(1)–O(4′)	117.47(6)

oxygen is supplied by the ethylene glycolate ligand, and the [dmae] group exists in two configurations, bidentate/chelating and monodentate/pendant.

The binuclear nature of (**1**) is unsurprising, as $Ti(OPr^i)_4$ has been reported[25] to exist principally as a dinuclear species in neat liquid form. The binuclear complexes $[Ti(OR)_3(acac)]_2$ (R = Me, Et, Pr^i) and $[Ti(OR)_3(thd)]_2$ (R = Me, Et, Pr^i), have also been structurally characterised,[26] and all contain six-coordinate Ti atoms in an octahedral configuration. The only

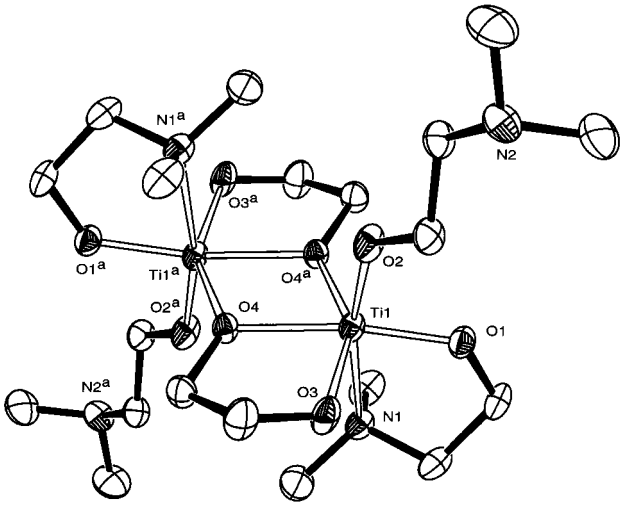

Fig. 1 Molecular structure of $[Ti(OCH_2CH_2O)(OCH_2CH_2NMe_2)_2]_2$, (**1**).

Ti–diolates which have been structurally characterised to date are $[Ti(OCH_2CH_2O)]_n$,[21] which is polynuclear with six-coordinate Ti atoms in a distorted octahedral environment, and the binuclear complex $[Ti(dmpd)_2]_2$,[22] which contains five-coordinate Ti atoms.

The bridging [Ti–O] bonds are longer (2.064(2) Å) than those not involved in bridging (1.8263(18)–1.8653(19) Å) and the [Ti–N] bond is the longest in the molecule at 2.409(2) Å. The alkoxide bridges are slightly asymmetric (Ti(1)–O(4) = 2.064(2), Ti(1)–O(4′) = 1.9880(17) Å), and a similar asymmetry has been noted in the bridging alkoxides in the binuclear complexes $[Ti(OR)_3(\beta\text{-diketonate})]_2$.[26]

The [Ti–O] bond lengths in (**1**), and trends in bond lengths, are very similar to those observed in other structurally characterised Ti–diolate complexes (see Tables 2 and 3), and are similar to the Ti–alkoxide bond lengths in a range of $[Ti(OR)_3(L)]_2$ dimeric complexes.[26]

The equatorial [O–Ti–O] bond angles all show a marked deviation from the ideal octahedral angles of 90°. The equatorial [O–Ti–O] bond angles vary from 70.86° to 106.52(9)°. The smallest [O–Ti–O] angle of 70.86(8)° is subtended by the oxygen atoms involved in bridging and the [O–Ti–O] bite angle of the ethylene glycolate ligand is also small (78.47(8)°), which has the effect of opening out the other [O–Ti–O] equatorial angles to 106.52(9)° and 101.43(9)°. The axial [N(1)–Ti(1)–O(2)] angle (168.15(9)°) also shows a marked deviation from the ideal value of 180°, and the [O–Ti–N] bite angle of the chelating dmae ligand is 74.98(8)°. The bond angles in (**1**) are compared with those in other Ti–diolate complexes in Table 3.

Complex (**2**) (Fig. 2) is also centrosymmetric and binuclear, but in this case the bridging oxygen atoms are provided by the [dmae] ligands, rather than the $[OCMe_2CMe_2O]$ diolate groups, presumably due to steric constraints. The [dmae]

Table 3 Selected bond lengths and angles for structurally characterised Ti–diolate complexes

	Bond lengths/Å			Bond angles/°		
Compound	Ti–O bridging	Ti–O non-bridging	Ti–Ti non-bonding	O–Ti–O bridging	O–Ti–O Diol "bite" angle	Reference
$[Ti(OCH_2CH_2O)(dmae)_2]_2$ (**1**)	2.064(2)	1.8263(18)–1.8653(19)	3.3019(5)	70.86(8)	78.46(8)	This work
$[Ti(OCMe_2CMe_2O)(dmae)_2]_2$ (**2**)	2.0128(13), 2.0909(13)	1.8131(15)–1.8768(14)	3.3398(4)	71.07(6)	80.05(6)	This work
$[Ti(OCH_2CH_2O)_2]_n$	2.004(1), 2.003(2)	1.837(2)	3.2724(6)	70.47(7)	78.49(7)	21
$[Ti(dmpd)_2]_2$	2.1375(18), 2.1528(17) 1.9572(16), 1.9542(16)	1.8015(19)–1.8366(19)		73.95(7), 74.36(7)	86.29(7), 86.86(8) 92.45(8), 92.81(9)	22

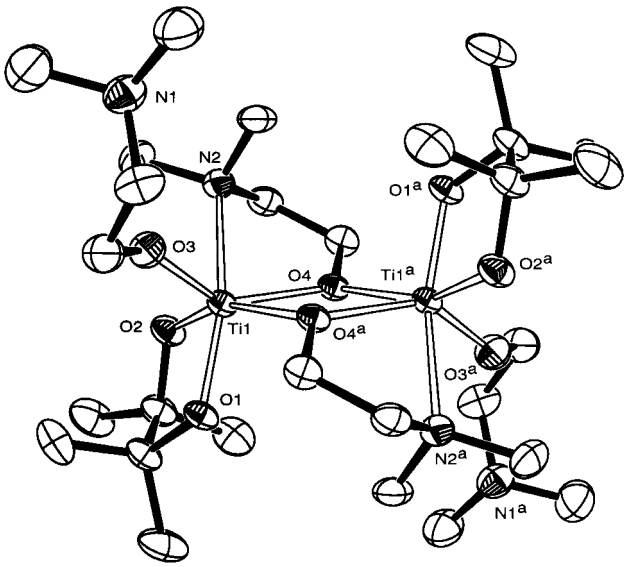

Fig. 2 Molecular structure of $[Ti(OCMe_2CMe_2O)(OCH_2CH_2NMe_2)_2]_2$, (**2**).

group exists in two configurations, monodentate and bidentate/chelating.

The non-bridging [Ti–O] bonds in (**2**) are shorter (1.8131(15)–1.8768(14) Å) than those involved in bridging (2.0128(13), 2.0909(13) Å), and the alkoxide bridges also show slight asymmetry. The [Ti–N] bond in (**2**) at 2.3041(17) Å is slightly shorter than the [Ti–N] bond in (**1**) (2.409(2) Å), but remains the longest bond in the molecule.

The $[TiO_5N]$ coordination sphere in (**2**) is a highly distorted octahedron. The equatorial [O–Ti–O] bond angles vary over the range 71.07(6)–139.26(6)°, markedly different from the ideal 90° angles. The smallest [O–Ti–O] angle of 71.07(6)° is subtended by the bridging oxygen atoms, and this leads to an opening out of the external [O(3)–Ti(1)–O(2)] and [O(3)–Ti(1)–O(4)] angles to 107.98(7) and 139.26(6)°, respectively. The bite angle of the $[OCMe_2CMe_2O]$ groups (80.05(6)°) is slightly greater than the bite angle of $[OCH_2CH_2O]$ in complex (**1**) (78.47(8)°).

The axial [N(2)–Ti–O(1)] angle of 158.50(6)° shows a significant deviation from the ideal 180° angle, and the [dmae] bite angle of 73.79(6)° is slightly less than the [dmae] bite angle in (**1**) (74.98(8)°). The bond lengths and angles in (**2**) are compared with those in other Ti–diolate complexes in Table 3.

MOCVD Of TiO_2

It was only found possible to deposit TiO_2 films reproducibly from complex (**2**). Despite repeated efforts, oxide growth from complex (**1**) was found to be inconsistent and was highly variable from run to run. In contrast, complex (**2**) allowed the reproducible deposition of TiO_2 thin films over the temperature range 325–450 °C, with and without added oxygen.

The atomic composition of the films was determined by Auger electron spectroscopy (AES) and the films were found to have O/Ti ratios of between 1.33 and 2.47, see Table 4. The O/Ti ratios in films deposited from (**2**) exhibit a wider range of values than previously observed in films grown from $[Ti(OPr^i)_2(dmae)_2]$ (O/Ti = 1.62–1.82) and $[Ti(OPr^i)_3(dmae)]$ (O/Ti = 1.62–1.74).[13] The high O/Ti ratio of 2.47 observed in film no. 3 (Table 4) can be attributed to the presence of interstitial oxygen, a relatively common phenomenon. It is however somewhat surprising that the film containing excess oxygen was grown in the absence of added O_2. Nitrogen was not detected (est. detection limit 1 atom%), but trace carbon was present in the majority of the films. The carbon is present in the bulk of the film and not as surface contamination and the carbon levels range from not detected up to 6 atom%, comparable to the levels found in TiO_2 films grown from $[Ti(OPr)_3(dmae)]$ (C = 2.9–7.7 atom%) and $[Ti(OPr^i)_2(dmae)_2]$ (C = 3.1–6.7 atom%).[13] Trace carbon is commonly observed in TiO_2 films grown by MOCVD from Ti–alkoxide precursors[27] and arises from the incomplete combustion of the metalorganic precursor. The carbon concentrations tend to decrease with increasing substrate temperature, a trend observed in films grown from $[Ti(OR)_4]$,[27] $[Ti(OPr^i)_3(dmae)]$[13] and $[Ti(OPr^i)_2(dmae)_2]$.[13] However, somewhat surprisingly the carbon levels appear not to be significantly influenced by the addition of oxygen. The optimum substrate temperature for TiO_2 layer purity, either with or without added oxygen, is 450 °C with no carbon detected in films grown at this temperature. The high purity of the films grown at 450 °C in the absence of oxygen indicates that complex (**2**) is an excellent "single-source" precursor to TiO_2 under optimised growth conditions.

The growth rate of the TiO_2 films varied from 43.5 to 208 nm h^{-1}. In films grown in the presence of oxygen, the optimum growth rate occurs at a substrate temperature of approximately 350 °C, slightly lower than the optimum substrate temperature of 400 °C reported for $[Ti(OPr^i)_3(dmae)]$ and $[Ti(OPr^i)_2(dmae)_2]$.

XRD analysis of films 2 and 8, grown at 400 °C (without O_2) and 450 °C (with O_2) respectively, showed that they are a polycrystalline mixture of the anatase phase (preferred orientation (004)) with a smaller amount of the rutile phase (preferred orientation (210)), see Fig. 3. This is consistent with other CVD studies which indicate that the anatase phase of TiO_2 is generally formed at substrate temperatures below 400 °C,[28] whilst TiO_2 in the rutile phase can be grown directly at temperatures above 500 °C.[29]

The reason for the marked difference in MOCVD behaviour between complexes (**1**) and (**2**) has not been established, but is likely to be due to structural differences between the two complexes. The main structural difference is that the [diolate] ligands in complex (**1**) bridge two Ti atoms, but are situated in

Table 4 Growth conditions[a] used to deposit TiO_2 thin films using $[Ti(OCMe_2CMe_2O)(OCH_2CH_2NMe_2)_2]_2$ (**2**)

Run No.	Ar flow rate/ $cm^3\ min^{-1}$	O_2 flow rate/ $cm^3\ min^{-1}$	Substrate temperature/°C	Film thickness[b]/ nm	Composition (atom%)			
					Ti	O	C	O : Ti ratio
1	1000	—	350		38.2	55.8	6.0	1.46
2^{XRD}	1000	—	400	208.0	41.7	55.4	2.9	1.33
3	1000	—	450		28.8	71.2	0	2.47
4	1000	150	325	43.5	39.7	56.7	3.6	1.43
5	1000	150	350		36.9	59.1	4.0	1.60
6	1000	150	400	50.0	39.2	56.9	3.9	1.45
7^{XRD}	1000	150	450	54.0	38.4	61.6	0.0	1.60
8	1000	100	350	60.0	40.5	55.3	4.2	1.36

[a]Evaporator temperature = 200 °C; Precursor injection rate = 3 $cm^3\ h^{-1}$; Duration of each run = 60 min; Si(100) substrates. [b]Estimated from AES data.

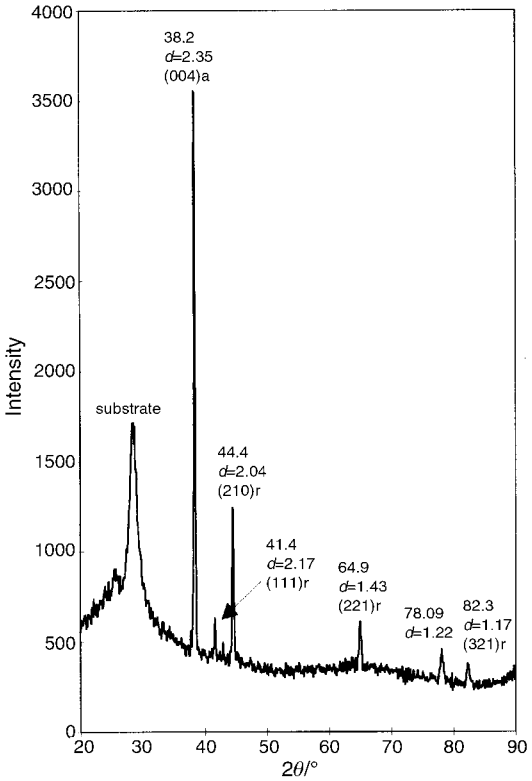

Fig. 3 XRD data for TiO_2 film deposited at 400 °C from (**2**) in the absence of oxygen: (a = anatase, r = rutile, d = d-spacing).

terminal positions in (**2**). It has been reported[18] that ethylene glycolate complexes of the type $[Ti(OCH_2CH_2O)(OR)_2]_2$ (R = Et, Pr^i, Bu^t) disproportionate on heating as shown in eqn. (1).

$$2[Ti(OCH_2CH_2O)(OR)_2]_2 \rightarrow Ti(OR)_4 + Ti(OCH_2CH_2O)_2 \quad (1)$$

Disproportionation reactions of this type are likely to be facilitated by bridging [diolate] ligands, as this configuration allows them to undergo an intramolecular rearrangement to chelate with one or other of the Ti atoms giving a $Ti(diol)_2$ species. Complex (**1**) may therefore be undergoing this disproportionation reaction in the heated evaporator and reactor inlet lines leading to pre-deposition of $[Ti(OCH_2CH_2O)_2]_n$, a polymeric low volatility material,[21] and the formation of $Ti(dmae)_4$. Although $Ti(dmae)_4$ has been used for the MOCVD of TiO_2,[15] it has been shown to deposit TiO_2 at relatively low temperature and was also found to be susceptible to gas phase pre-reactions. These earlier studies were carried out at reduced pressure (1 Torr), which would minimise pre-deposition of TiO_2. However, the present MOCVD study was carried out at atmospheric pressure, conditions in which $Ti(dmae)_4$ is likely to have an increased tendency to pre-reaction. Decomposition of $Ti(dmae)_4$ in the reactor inlet pipes would lead to extensive depletion of Ti precursor species from the gas phase and preclude TiO_2 growth. The presence of a significant amount of white deposit at the reactor inlet supports this proposal. The disproportionation reaction is likely to occur to a varying extent depending on the specific growth conditions, which may explain the highly irreproducible behaviour of (**1**) in MOCVD.

The ^1H NMR spectrum of complex (**1**) is relatively simple and does not distinguish between unidentate and chelating [dmae] ligands, indicating that the complex is fluxional in solution at room temperature, and this further increases the possibility of a redistribution of the type shown in eqn. (1).

In contrast, due to the steric demands of $[OCMe_2CMe_2O]$, the pinacolate ligands are located in terminal positions in complex (**2**), and there is thus no longer a ready pathway to the formation of $Ti(diol)_2$ *via* an intramolecular disproportionation reaction. This is supported by the ^1H NMR data for (**2**) which does differentiate between the separate [dmae] ligands in the complex, indicating that the dimeric configuration is largely maintained in solution, effectively precluding the intramolecular redistribution of the terminal [diolate] ligands. Consequently, on heating in the evaporator (**2**) is likely to dissociate in a symmetric fashion to give the volatile Ti–alkoxide species $[Ti(OCMe_2CMe_2O)(dmae)_2]$ which subsequently lead to the reproducible deposition of TiO_2.

In the absence of detailed *in situ* mechanistic studies, the growth mechanisms proposed above remain speculative, however the proposed mechanism is supported by the observation that the liquid complex $[Ti(mpd)(dmae)_2]_2$ (mpd = 2-methylpentane-2,4-diolate) also allows the reproducible deposition of TiO_2 films by liquid injection MOCVD.[30] The complex is likely to be dimeric, as mpd, like pinacol, is sterically demanding and so is likely to be situated in terminal positions, inhibiting the disproportionation reaction shown in eqn. (1).

TGA data on (**1**) and (**2**) also provides some support for the disproportionation mechanism. Complex (**1**) exhibits a complicated TGA trace, with five regions of weight loss in the temperature region 0–400 °C, together with two further regions of weight loss between 400 and 600 °C, and a large residue remains after evaporation. This is consistent with the formation and evaporation of a number of species during heating, which would be formed in a disproportionation reaction. In contrast, the TGA data for (**2**) shows that the complex evaporates in a simple evaporation process in the temperature range 0 to 350 °C.

4. Conclusions

The complexes $[Ti(OCH_2CH_2O)(OCH_2CH_2NMe_2)_2]_2$ (**1**) and $[Ti(OCMe_2CMe_2O)(OCH_2CH_2NMe_2)_2]_2$ (**2**) have been shown to be dimeric by X-ray diffraction, but have marked structural differences which may account for their significantly different behaviour in liquid injection MOCVD.

Acknowledgements

P.A.W. would like to thank Inorgtech Limited for provision of a fully funded post-doctoral studentship. We are also grateful to Mr S. Apter for the microanalysis data.

References

1 D. E. Putzig and T. W. del Pesco, in *Kirk Othmer Encyclopedia of Chemical Technology*, Wiley, New York, 1997, vol. 24, p.322.
2 R. O. Duthaler and A. Haffner, *Chem. Rev.*, 1992, **92**, 807.
3 T. Mallat and A. Baiker, *J. Catal.*, 1995, **153**, 177.
4 J. Livage, M. Henry and C. Sanchez, *Prog. Solid State Chem.*, 1988, **18**, 259, and references therein.
5 M. M. Yokazawa, H. Iwasa and I. Teramoto, *Jpn. J. Appl. Phys.*, 1968, **7**, 96.
6 C. H. Peng and S. B. Desu, *J. Am. Ceram. Soc.*, 1994, **77**, 1799.
7 *Ferroelectric Thin Films IV*, ed. B. A. Tuttle, S. B. Desu, R. Ramesh and T. Shiosaki, *Mater. Res. Soc. Symp. Proc.*, 1995, **361**, and references therein.
8 S. Doeuff, M. Henry, C. Sanchez and J. Livage, *J. Non-Cryst. Solids*, 1987, **89**, 206.
9 T. Kemmitt and M. Daglish, *Inorg. Chem.*, 1998, **37**, 2063.
10 A. C. Jones, T. J. Leedham, P. J. Wright, M. J. Crosbie, P. A. Lane, D. J. Williams, K. A. Fleeting, D. J. Otway and P. O'Brien, *Chem. Vap. Deposit.*, 1998, **4**, 46.
11 J. F. Roeder, B. A. Vaartstra, P. C. Van Buskirk and H. R. Beratan, *Mater. Res. Soc. Symp. Proc.*, 1996, **415**, 123.
12 D. B. Beach and C. E. Vallet, *Mater. Res. Soc. Symp. Proc.*, 1996, **415**, 225.
13 A. C. Jones, T. J. Leedham, P. J. Wright, M. J. Crosbie,

K. A. Fleeting, D. J. Otway, P. O'Brien and M. E. Pemble, *J. Mater. Chem.*, 1998, **8**, 1773.
14 C. Jimenez, M. Paillous, R. Madar, J. P. Senateur and A. C. Jones, *J. Phys. IV Fr.*, 1999, **9**, Pr8–569.
15 J.-H. Lee, J.-Y. Kim, J.-Y. Shim and S.-W. Rhee, *J. Vac. Sci. Technol.*, 1999, **A17**, 3033.
16 J.-H. Lee and S.-W. Rhee, *J. Mater. Res.*, 1999, **14**, 3988.
17 C. O. Bostwick, *US Patent*, 2,643,262, 1953 (*Chem. Abstr.*, 1954, **48**, 5203).
18 D. M. Puri and R. C. Mehrotra, *Indian J. Chem.*, 1967, **5**, 448.
19 G. H. Dahl and B. P. Block, *Inorg. Chem.*, 1966, **5**, 1395.
20 A. Yamamoto and S. Kambara, *J. Chem. Soc.*, 1959, 2663.
21 D. Wang, R. Yu, N. Kumada and N. Kinomura, *Chem. Mater.*, 1999, **11**, 2008.
22 S. M. Damo, K.-C. Lam, A. Rheingold and M. A. Walters, *Inorg. Chem.*, 2000, **39**, 1635.
23 G. M. Sheldrick, SHELX-97, Programs for Crystal Structure Solution and Refinement, University of Göttingen, Germany, 1997.
24 A. C. Jones, T. J. Leedham, P. J. Wright, M. J. Crosbie, P. A. Lane, D. J. Williams, K. A. Fleeting, D. J. Otway and P. O'Brien, *Chem. Vap. Deposit.*, 1998, **4**, 46.
25 S. M. Damo, K.-C. Lam, A. Rheingold and M. A. Walters, *Inorg. Chem.*, 2000, **39**, 1635.
26 R. J. Errington, J. Ridland, W. Clegg, R. A. Coxall and J. M. Sherwood, *Polyhedron*, 1998, **17**, 659.
27 T. Won, S. Yoon and H. Kim, *J. Electrochem. Soc.*, 1992, **139**, 3284.
28 N. Rausch and E. P. Burte, *J. Electrochem. Soc.*, 1993, **140**, 145.
29 M. Ritala, M. Leskala, E. Nykanen, P. Soininen and L. Niinisto, *Thin Solid Films*, 1993, **225**, 288.
30 A. Awaluddin, M. E. Pemble, A. C. Jones and P. A. Williams, paper submitted to EURO CVD 13, Athens, August 2001.